Geophysical Research Letters

RESEARCH LETTER
10.1029/2020GL091094

Key Points:

- Temperature and oxygen data from four fjords (Rivers, Knight, and Bute Inlets and Douglas Channel) from 1951 to 2020 were examined
- Over 70 years, deep water has warmed by up to 1.3°C and lost up to 0.7 mLL^{-1} of oxygen, with evidence of accelerated warming since 2016
- Deep warming and deoxygenation trends are statistically alike in at least three of the four fjords, suggesting similar drivers

Supporting Information:

- Supporting Information S1

Correspondence to:

J. M. Jackson,
jennifer.jackson@hakai.org

Citation:

Jackson, J. M., Bianucci, L., Hannah, C. G., Carmack, E. C., & Barrette, J. (2021). Deep waters in british Columbia mainland fjords show rapid warming and deoxygenation from 1951 to 2020. *Geophysical Research Letters*, *48*, e2020GL091094. https://doi.org/10.1029/2020GL091094

Received 2 OCT 2020
Accepted 8 JAN 2021

Deep Waters in British Columbia Mainland Fjords Show Rapid Warming and Deoxygenation From 1951 to 2020

Jennifer M. Jackson[1], Laura Bianucci[2], Charles G. Hannah[2], Eddy C. Carmack[2], and Jessy Barrette[1]

[1]Hakai Institute, Victoria, BC, Canada, [2]Institute of Ocean Sciences, Fisheries and Oceans Canada, Sidney, BC, Canada

Abstract Many complex fjord systems cross British Columbia's coastline. A 70 year (1951–2020) time series analysis of temperature, salinity, and oxygen in four such fjords between ~54 and 50°N (Douglas Channel, Rivers Inlet, Knight Inlet and Bute Inlet) shows that changes were greatest in deep waters between the sill and the bottom. In Rivers, Knight and Bute Inlet, the deep water temperature increased by 1.2–1.3°C over 70 years, up to two times the global average for open ocean waters at corresponding depths, while salinity increased by 0.1–0.2, and oxygen decreased by 0.4–0.7 mLL^{-1}. The most northern inlet, Douglas Channel, showed a temperature increase of 0.8°C from 1951 to 2016, while trends in oxygen and salinity were not statistically significant. An analysis of Apparent Oxygen Utilization suggests that the deep waters in Douglas Channel are more readily exchanged with the outer coast than the three other fjords.

Plain Language Summary Glacially carved fjords draw their deep waters from adjacent offshore ocean basins through a combination of upwelling, cross-shelf transport, tidal mixing and estuarine circulation related processes. We studied data spanning seven decades from four such systems covering four degrees of latitude along the Canadian Pacific and found that fjord deep waters below sill depth were warming two times faster than their offshore source waters. Changes in temperature were accompanied by significant trends of decreased oxygen concentrations and increased salinity. Potential processes explaining these anomalous responses to climate change are discussed.

1. Introduction

Fjords are formed by glacial erosion and retreat, leaving behind a terminal moraine or sill at their mouth (Farmer & Freeland, 1983; Pickard, 1961). Fjords are fed by rivers and streams that transport freshwater and land-derived material properties such as dissolved (Oliver et al., 2017) and particulate organic carbon (St Pierre et al., 2020). Fjords often serve as a gateway between fresh and marine waters for anadromous fish species such as salmon and eulachon (see Bianchi et al., 2020).

Recent studies have documented changes to the world's fjords. In Chilean Patagonia, a southward displacement of upwelling-favorable winds by 11 km year^{-1} from 2003 to 2016 (Narvaez et al., 2019) could impact fjord reoxygenation (Silva & Vargas, 2014). In Northeast Greenland, coastal freshening from glacial melt has constrained deep water renewal of Young Sound-Tyrolerfjord (Boone et al., 2018). In Norway, warming of North Atlantic water has reduced the rate of deep-water renewal and increased deoxygenation of Masfjorden (Aksnes et al., 2019). In British Columbia, anomalously warm water from the 2014 to 2016 marine heatwave lingered in deep water of Rivers Inlet through at least 2018 (Jackson et al., 2018). Thus, at global scales, climate change is impacting fjords.

Rivers Inlet, Knight Inlet, Bute Inlet, and Douglas Channel (Figure 1) are fjords on British Columbia's mainland central coast, with glacial watersheds at their heads. Importantly, each fjord has a different connection pathway to the open ocean—Douglas Channel is a complex series of inlets with two entrances to the open ocean via Hecate Strait, Rivers Inlet faces the open ocean via Queen Charlotte Sound, Knight Inlet connects to the open ocean through Queen Charlotte Strait and the Broughton Archipelago, and Bute Inlet connects to the open ocean through Juan de Fuca Strait and the Strait of Georgia. This is the first time that a time series of temperature, salinity, and oxygen dating back to 1951 for multiple locations on the BC coast has been jointly examined in the context of climate change.

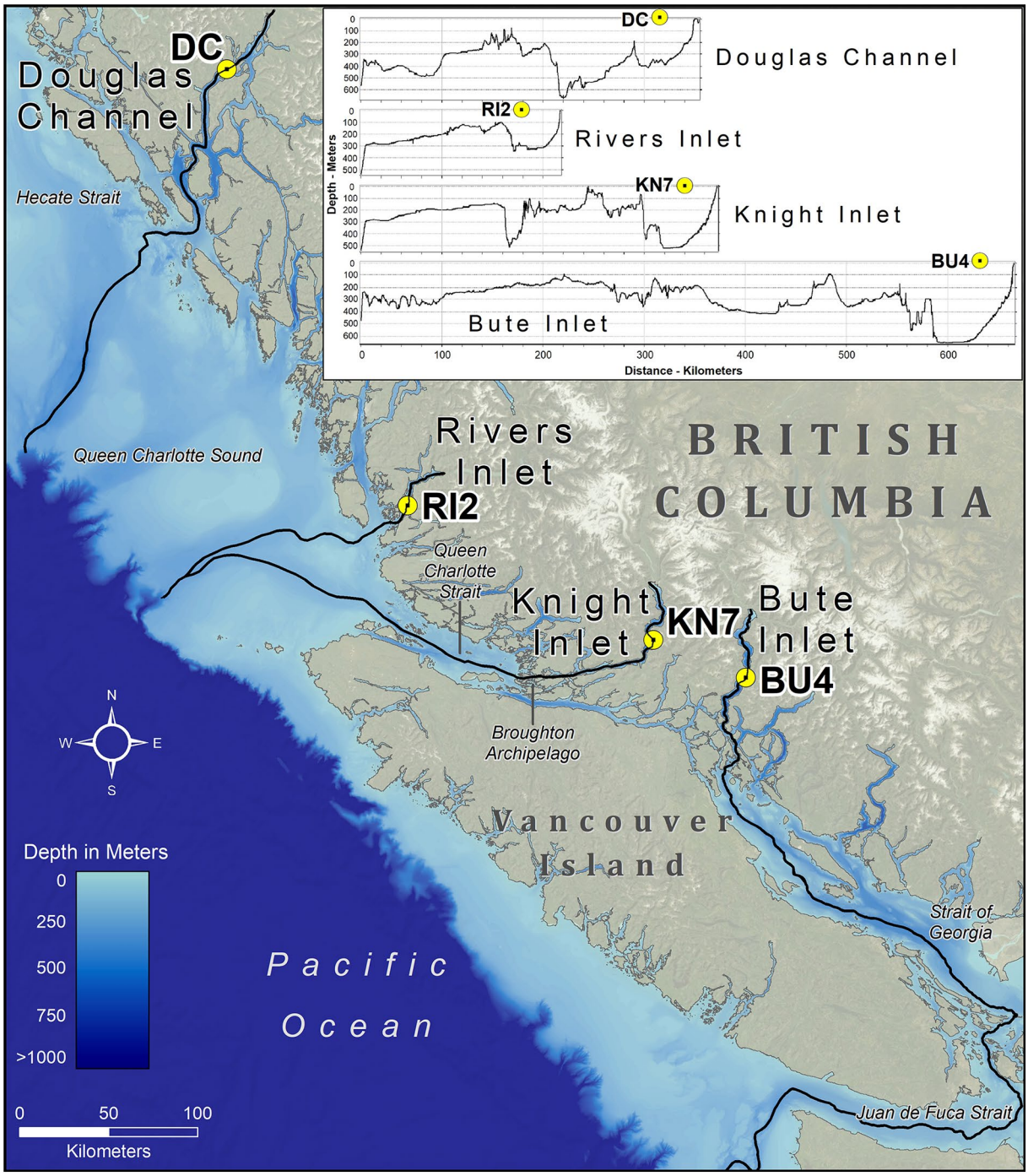

Figure 1. Bathymetric map of British Columbia's central coast, highlighting station DC in Douglas Channel, station RI2 in Rivers Inlet, station KN7 in Knight Inlet, and station BU4 in Bute Inlet. Bathymetric data starting at offshore 200 m isobath (from https://www.ncei.noaa.gov) along the black lines are shown in inset for each station.

2. Data and Methods

2.1. Data

Temperature, salinity, and oxygen measurements have been collected in our study area since 1951 (Figure S1) through independent programs by the University of British Columbia, Fisheries and Oceans Canada, and the Hakai Institute (Table S1). We examined one station in each inlet—DC (Douglas Channel), RI2

(Rivers Inlet), KN7 (Knight Inlet), and BU4 (Bute Inlet), which were selected because they were located landward of the fjord's entrance sill (~120 km from the entrance sill for DC, ~20 km for RI2, and ~50 km for KN7 and BU4), and in a deep basin (Figure 1). In total, 411 CTD profiles were examined—31 from DC, 162 from RI2, 97 from KN7, and 121 from BU4. Since data were collected using different methods, we follow Chandler et al. (2017) and interpret the temperature, salinity, and oxygen data to an accuracy of 0.1°C, 0.1 salinity units, and 0.1 mLL^{-1}, respectively. The temporal distribution of data collected at each station varied according to observational program (Figure S1; Table S1). For all data, the seasonal cycle was removed as reported in the supplementary information.

Trendlines for the different variables at each station were computed using ordinary least squares. The trends were compared against each other using a z-test, where the z-score (z) was calculated as $z = (A-B)/\mathrm{sqrt}(SE\_A^2+SE\_B^2)$ where A was the slope of the first trendline, B was the slope of the second trendline, and SE_ was the standard error of the slope. The null hypothesis (i.e., the assumption that the two slopes are statistically the same) was rejected at 95% if $z > 1.96$ or $z < -1.96$.

2.2. Water Types

We define three water types for the inlets. The first is surface water, which is water lighter than a potential density of 1,022 kgm^{-3}. The second is intermediate water, which starts at the base of surface water (typically less than 10 m) and ends at the sill depth, which is (following Pickard, 1961 and Wan et al., 2017) 200 m in Douglas Channel, 137 m in Rivers Inlet, 64 m in Knight Inlet, and 355 m in Bute Inlet. The third is deep water, which starts at the sill depth and ends at the bottom, such that deep water is 201–370 m at station DC, 137–334 m at station RI2, 65–513 m at station KN7, and 356–632 m at station BU4 (Pickard, 1961). The average temperature, salinity, and oxygen (DO) within each water type were calculated for each profile; we here focus on deep water because this is where the largest changes were observed.

2.3. Calculation of Temperature Impact on Oxygen Changes

Temperature variability affects oxygen concentrations, so the dissolved oxygen saturation (DOsat) was calculated using the TEOS-10 Matlab toolbox (www.teos-10.org) applied to in situ temperature and salinity data. Afterward, the seasonal cycle was removed as described in the supplemental information. Following the regional literature (Baker & Pond, 1995; Hodal, 2010; Lafond & Pickard, 1975; Wan et al., 2017), it was assumed that deep water was renewed annually in each fjord.

To remove the effect of temperature and solubility from DO changes, apparent oxygen utilization (AOU = DOsat – DO) was calculated, which represents the change in oxygen since a water parcel was last in contact with the atmosphere (e.g. Pytkowicz, 1971; Broecker & Peng, 1982), and assumes the surface oxygen concentration was DOsat (e.g., Ito et al., 2004). AOU estimates biological processes, with positive values indicating aerobic remineralization that consumes DO and negative values indicating photosynthesis that produces DO. Mixing and advection can affect DO and DOsat, so impact the value of AOU (Koeve & Kähler, 2016). To distinguish between in situ biological processes and mixing, we follow Pytkowicz (1971) and plot AOU against salinity for the deep waters of the fjords; a linear relationship indicates that changes in AOU result from mixing rather than local remineralization/photosynthesis. For example, if two water masses are mixed in the absence of local biological processes, the final values of both AOU and salinity are simply a weighted average of the source waters' AOU and salinities. In an AOU versus S plot, AOU_{final} and S_{final} fall on top of the line that connects water masses 1 and 2 end points. However, if there is *in situ* remineralization, the final AOU will change at a different proportion than S and will introduce nonlinearity in the AOU versus S space.

3. Results

Deep waters in all four fjords revealed statistically significant trends, based on the trendline, from 1951 to 2020 of increasing temperature (Figure 2a), resulting in decreased DOsat (Figure 3b). In Rivers, Knight and Bute Inlet, salinity significantly increased (Figure 2b) and DO significantly decreased (Figure 3a). Only in Bute Inlet did AOU significantly increase (Figure 3c). Table 1 shows several metrics, including slopes, p

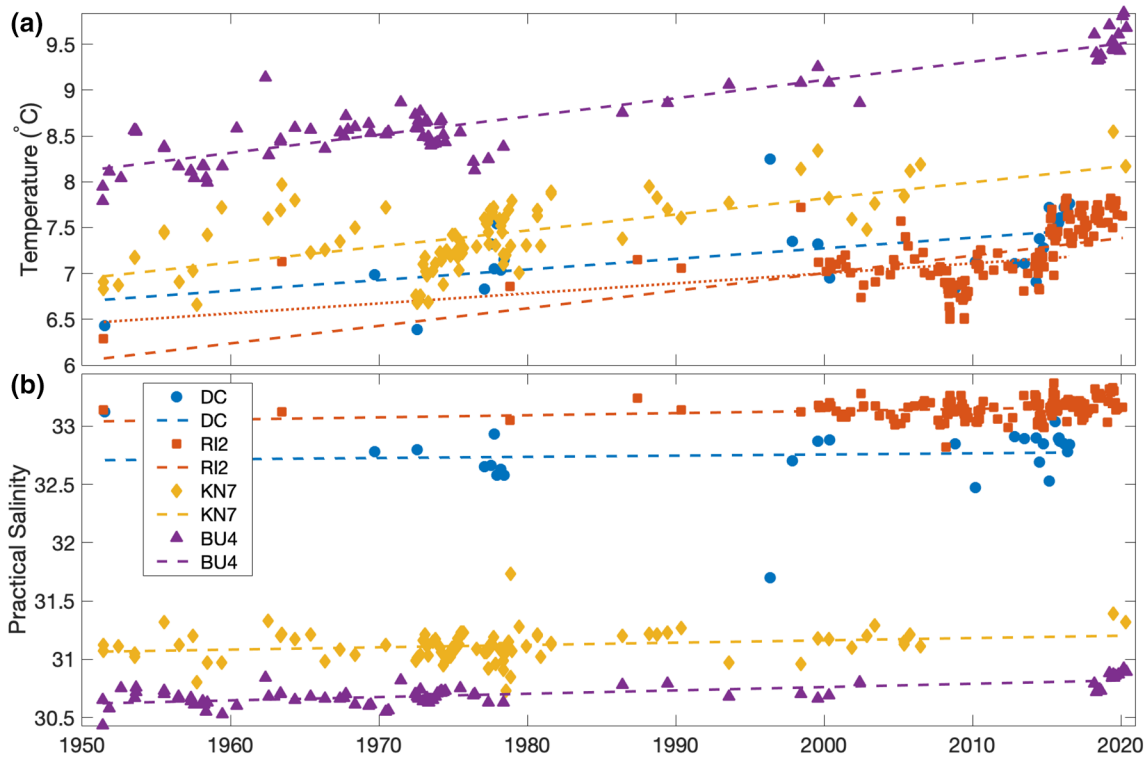

Figure 2. (a) Temperature and (b) practical salinity in deep water at DC (Douglas Channel), RI2 (Rivers Inlet), KN7 (Knight Inlet) and BU4 (Bute Inlet) from 1951 to 2020. The seasonal cycle was removed as described in the supplementary material. The dashed lines represent the linear best fit for each station (statistics are reported in Table 1). The dotted orange line represents the linear best fit for station RI2 from 1951 to July 2016, the same length of time as the DC time series.

values, determination coefficient, and the total change from 1951 to 2020 (based on the trendlines). Deoxygenation, salinity, temperature, and DOsat trends are statistically indistinguishable at 95% confidence for the three southern inlets.

The Douglas Channel time series ended in 2016 and in 2020 at the other inlets. To determine the impact of the shorter time series, we examined temperature in Rivers Inlet from 1951 to 2016 (Knight and Bute Inlets had large data gaps through the 1990s) and found that trend lines were almost identical to Douglas Channel (Figure 2a), suggesting similar warming in Rivers Inlet and Douglas Channel from 1951 to 2016. In addition, the slope of the temperature line was steeper in Rivers Inlet (1951–2020) than Douglas Channel (1951–2016; Figure 2a and Table 1), suggesting that warming has accelerated since 2016. We acknowledge that the large data gaps in Rivers Inlet are a potential source of error; however, z-tests show that the slope of the lines are statistically similar in all inlets, suggesting that the trend in Rivers Inlet is real. Further, boxplots of temperature and oxygen at decadal scale were constructed in all four inlets (Figures S3 and S4) and they showed that, based on a z-test, the trends calculated from the decadal median temperature and oxygen were statistically similar to the trends shown in Figures 2 and 3 in all inlets, except for DO in Rivers Inlet (Table S2).

Hypoxic conditions, here taken as oxygen concentrations below 2 mLL^{-1} (e.g., Diaz & Rosenberg, 2008), have been observed in the deep water of Rivers and Bute Inlet but not in Knight Inlet or Douglas Channel. In Rivers Inlet, hypoxic deep water was observed in March 2009, 2014 to 2017, and 2019 and in April 2014, 2016, and 2019. In Bute Inlet, available data shows hypoxic deep waters in June 1998, July 1999, and March and July 2018. These two inlets show the overall lowest mean DO concentrations (Figure 3a), which combined with the observed trends in deoxygenation, leads to the observed hypoxic conditions.

AOU is positive at all four stations (Figure 3c), suggesting that consumption of DO, via biological processes, is occurring. The increasing AOU indicates that DO changes are larger than DOsat changes (i.e., DO

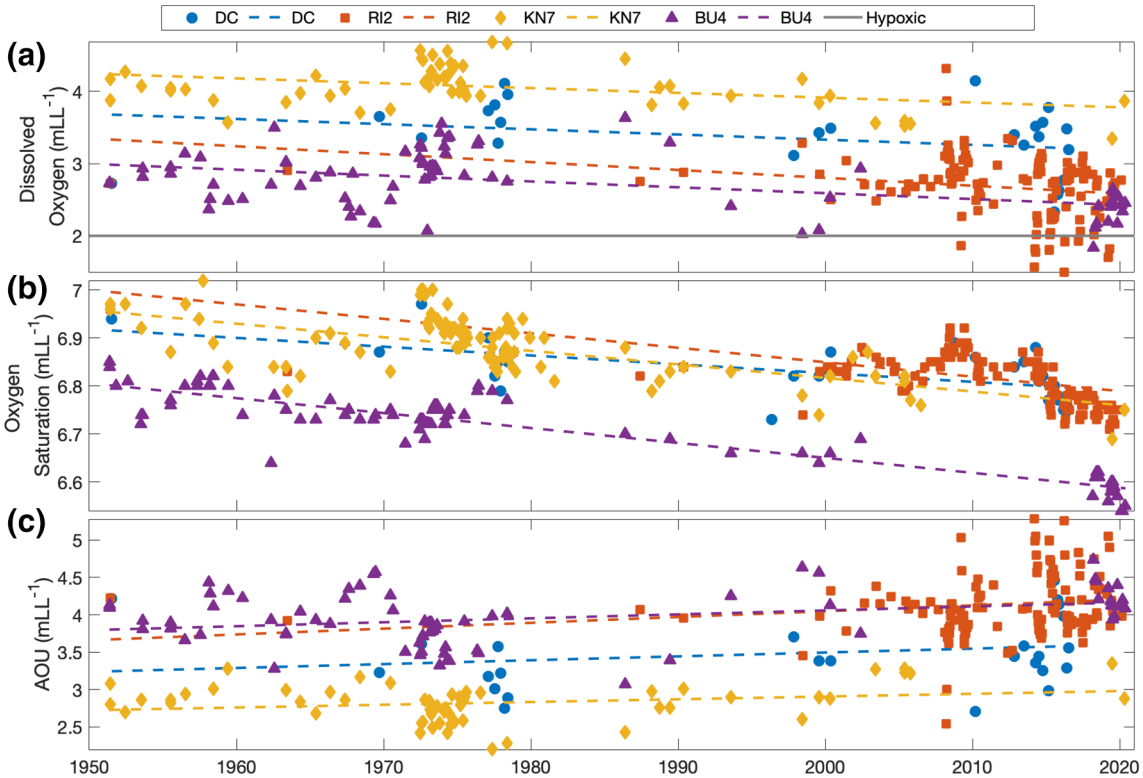

Figure 3. As in Figure 4 but for (a) dissolved oxygen (DO), (b) oxygen saturation (DOsat), and (c) apparent oxygen utilization (AOU) in deep water (all in mLL^{-1}). Horizontal gray line in top panel highlights the hypoxic threshold (2 mLL^{-1}).

decreases faster than DOsat; see Table 1); these trends are significant in the three southern inlets (at 95% confidence with $p < 0.05$ in Bute Inlet; Rivers and Knight Inlets would be significant at 90% with $p < 0.1$), suggesting that decreased oxygen solubility due to warmer waters is not the only driver of deoxygenation in these three fjords (more detail in Section 4.2).

A plot of AOU versus salinity shows different roles of water mass mixing versus *in situ* remineralization in the different fjords (Figure 4; see details about this kind of plot in Section 2.3). The relationship is significantly linear in Douglas Channel ($r^2 = 0.62$, $p << 0.01$); however, in Rivers and Knight Inlet, a linear regression explains little variability ($r^2 = 0.15$ and 0.19, respectively, both with $p << 0.01$), while it explains none in Bute Inlet ($r^2 \approx 0.00$, $p = 0.64$). Bute has a stronger relationship between temperature (and thus, DOsat) and salinity, whereas DO versus salinity dominates the AOU slope in the other three fjords (Figure S5).

4. Discussion

Multidecadal time series of deep-water properties in three different British Columbia mainland fjords have shown, despite data gaps, statistically significant increases in temperature and salinity and decreases in oxygen, while a fourth, Douglas Channel, showed significant trends in temperature only. The fact that the warming and deoxygenation trends are statistically similar in the three southerly fjords infers that common processes are driving the changes; we note, however, that differences exist between the northern Douglas Channel and the three southern fjords.

4.1. Mechanisms for Warming

A recent assessment of 2004–2019 global ocean data by Johnson et al., (2020) found that waters at 150 m (about the depth of source water) are warming on average 0.1ºC per decade. At Ocean Station Papa in the northeast Pacific Ocean, using data from 1956 to 2011, Freeland (2013) reported a warming trend of 0.05ºC

Table 1
Regression Slopes (With Standard Error) and Associated Metrics (p-value and r^2 Value) for Time Series From 1951 to 2020 at Deep Waters of the Four Stations

	DC	RI2	KN7	BU4
Temperature (ºC/decade)	**Slope = 0.12 ± 0.035**	**Slope = 0.19 ± 0.027**	**Slope = 0.18 ± 0.022**	**Slope = 0.20 ± 0.010**
	p = 0.0025	**p < 0.0001**	**p < 0.0001**	**p < 0.0001**
	r^2 = 0.30	**r^2 = 0.26**	**r^2 = 0.40**	**r^2 = 0.83**
	Δ = 0.8ºC	**Δ = 1.3ºC**	**Δ = 1.2ºC**	**Δ = 1.3ºC**
Salinity (salinity units/decade)	Slope = 0.01 ± 0.026	**Slope = 0.02 ± 0.008**	**Slope = 0.02 ± 0.009**	**Slope = 0.03 ± 0.003**
	p = 0.7019	**p = 0.0315**	**p = 0.0364**	**p < 0.0001**
	r^2 = 0.01	**r^2 = 0.04**	**r^2 = 0.05**	**r^2 = 0.48**
		Δ = 0.2	**Δ = 0.1**	**Δ = 0.2**
Oxygen (mLL^{-1}/decade)	Slope = −0.07 ± 0.047	**Slope = −0.11 ± 0.043**	**Slope = −0.07 ± 0.023**	**Slope = −0.08 ± 0.019**
	p = 0.1424	**p = 0.013**	**p = 0.0053**	**p < 0.0001**
	r^2 = 0.09	**r^2 = 0.05**	**r^2 = 0.13**	**r^2 = 0.19**
		Δ = −0.7 mLL^{-1}	**Δ = −0.4 mLL^{-1}**	**Δ = −0.6 mLL^{-1}**
Oxygen saturation (mLL^{-1}/decade)	**Slope = −0.02 ± 0.005**	**Slope = −0.03 ± 0.004**	**Slope = −0.03 ± 0.004**	**Slope = −0.03 ± 0.002**
	p = 0.0005	**p < 0.0001**	**p < 0.0001**	**p < 0.0001**
	r^2 = 0.38	**r^2 = 0.27**	**r^2 = 0.39**	**r^2 = 0.82**
	Δ = −0.1 mLL^{-1}	**Δ = −0.2 mLL^{-1}**	**Δ = −0.2 mLL^{-1}**	**Δ = −0.2 mLL^{-1}**
Apparent oxygen utilization (mLL^{-1}/decade)	Slope = 0.05 ± 0.047	Slope = 0.07 ± 0.042	Slope = 0.04 ± 0.000	**Slope = 0.05 ± 0.018**
	p = 0.2781	p = 0.0671	p = 0.0734	**p = 0.0051**
	r^2 = 0.05	r^2 = 0.03	r^2 = 0.06	**r^2 = 0.10**
				Δ = 0.4 mLL^{-1}

Note. Changes observed were positive for temperature (warming), salinity (salinification), and AOU and negative for oxygen (deoxygenation). Slopes and their errors are shown in units of the variable (ºC for temperature, mLL−1 for oxygen) per decade. Statistically significant relationships, here defined as when the p-value for a linear relationship is less than 0.05, are highlighted in bold. In the latter cases, the total change Δ from 1951 to 2016 or 2020 (based on the trendline) is given.

per decade at 200 m, which increased to 0.08ºC per decade at 150 m when the timeseries was extended to 2018 (Cummins & Ross, 2020). Within deep water, we observed a warming rate of 0.12°C per decade in Douglas Channel, 0.19°C per decade in Rivers Inlet, 0.18°C per decade in Knight Inlet, 0.20°C per decade in Bute Inlet. This rate is 1–2 times the global average found by Johnson et al. (2020), about 3 times the warming rate reported by Freeland (2013), and twice the warming rate reported by Cummins and Ross (2020). Why, then, are the deep waters in these fjords warming at a greater rate than the open ocean?

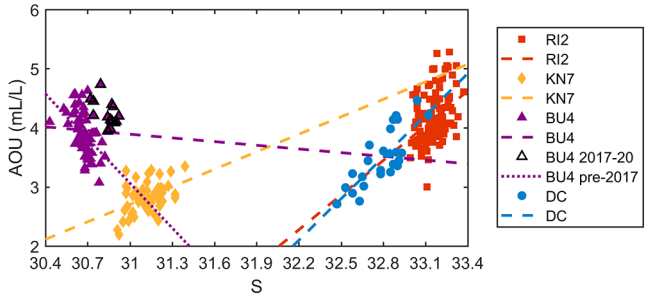

Figure 4. Apparent oxygen utilization versus salinity in deep waters of the four fjord stations (color scales as in previous figures). The dashed lines represent the linear best fit for each station. Data at BU4 from 2017 onwards is highlighted in black symbols, and a linear fit without these data is shown by the dotted line for BU4 only.

Upwelling causes deep-water renewal in all four inlets (Baker & Pond, 1995; Hodal, 2010; Lafond & Pickard, 1975; Wan et al., 2017). Upwelled water travels from the NE Pacific to Rivers Inlet along the 1,026 kgm^{-3} isopycnal (Hare et al., 2020) and both offshore and deep Rivers Inlet water were anomalously warm following the 2014–2016 marine heatwave (Jackson et al., 2018; Scannell et al., 2020), which accelerated the warming trend after 2016 (Figure 2a and Table 1). Rivers Inlet deep water is significantly denser than waters in Bute or Knight Inlet, yet the fact that some of the warmest deep waters in Bute and Knight Inlet were observed after 2017 suggests that, similar to Rivers Inlet, the source waters for Bute and Knight Inlet also warmed. Once deep water enters a fjord and is trapped behind the sill (Farmer & Freeland, 1983), it is modified only by slow processes such as vertical eddy diffusion (Pawlowicz, 2017) or yearly deep-water renewal events. Since the offshore

source of upwelled water remained anomalously warm through at least 2018 (Jackson et al., 2018), fjord deep water continued to be anomalously warm. Furthermore, winter outflow winds cool fjord waters (MacNeil, 1974), and winter continental temperatures are warming by more than 2°C per century (BC Ministry of Environment, 2016), so it is possible that continental warming has meant less cooling of fjord water.

4.2. Mechanisms for Deoxygenation

The DO changes we observe in fjord deep waters are like those observed in the northeast Pacific Ocean. Cummins and Ross (2020) found a deoxygenation trend from 1956 to 2020 of about 0.5 mLL^{-1} (0.09 mLL^{-1}per decade) at 150 m in the open ocean Station Papa, which is similar to the deoxygenation we observed in fjord deep waters (0.07–0.11 mLL^{-1} per decade (Table 1). It is important to note that oxygen over the continental slope of the northeast Pacific has oscillated from low concentrations in the 1950s to high concentrations in the 1980s and back to low concentrations in the 2010s (Crawford & Peña, 2016), and thus these results should be interpreted within the context of multidecadal oscillations. Waters from about 150 m in the northeast Pacific are the source for deep water in Rivers Inlet (Jackson et al., 2018); thus, it is likely that much of the deoxygenation observed in deep fjord waters are associated with changes in source waters from the northeast Pacific. Other processes that can impact oxygen concentrations in fjord deep waters are examined below.

The comparison of changes in DOsat from 1951 to 2020 (0.2 mLL^{-1} for the three inlets) to those of DO (0.8, 0.5, and 0.6 mLL^{-1} for Rivers, Knight, and Bute Inlet) suggests that temperature-dependent solubility effects (either locally or at the source waters) represent 28%, 42%, and 39% of the total DO change in each of those three inlets, respectively. Since the fjord deep water is warming faster than offshore water, it is likely that the decreased solubility in coastal fjords, which enhances deoxygenation, plays a more important role in these coastal waters than offshore (e.g. Crawford & Peña, 2016).

Warmer waters accelerate aerobic remineralization (i.e., the decomposition of organic matter by oxygen-consuming bacteria), leading to a stronger sink of DO by bacteria (e.g. Brewer & Peltzer, 2017; Pomeroy & Wiebe, 2001). The remineralization rate ($r(T)$) can be estimated if we assume a typical Q_{10} formulation for this process (e.g. Peña et al 2016; Segschneider & Bendtsen, 2013),

$$r(T) = r_0\, Q_{10}^{\frac{T-T_0}{10}}$$

where Q_{10} is the rate change for a 10K temperature increase and r_0 is the remineralization rate at a reference temperature T_0. If we apply the above equation to two temperatures, T_1 and $T_1 + \Delta T$, we find that $Q_{10}^{\Delta T/10}$ represents the fractional change due to a temperature change ΔT. Typical values of Q_{10} vary between 1.5 and 3 (e.g., Lomas et al., 2002; López-Urrutia et al., 2006; Laufkötter et al., 2017), with $Q_{10} = 2$ a conservative estimate of the temperature sensitivity (Segschneider & Bendtsen, 2013). Applying the change in temperature found in the three southern inlets (1.2°C–1.3°C), we estimate that the effect of warming on remineralization rates is around 9% (varying between 5% and 15% if we use a Q_{10} of 1.5 or 3, respectively). This suggests that increased remineralization under observed warming conditions have had a quantifiable effect on deoxygenation in fjord deep waters.

Increased primary production and rainout of organic matter to the deep water can also enhance the total amount of remineralization, but unfortunately only Rivers Inlet has a useful chlorophyll timeseries, starting in 2014. The analysis of a 2014–2018 time series of vertically integrated chlorophyll from 5 to 50 m depth shows a decline in the magnitude of the spring bloom in this station (Jackson et al, under revision). This suggests increased rainout is not a mechanism for deoxygenation in the deep waters. However, this short chlorophyll time series prevents us from making a sound conclusion in the context of our longer DO time series.

Our analysis of AOU versus salinity following Pytkowicz (1971) highlights some differences between Douglas Channel and the southern inlets. Specifically, changes in AOU in Douglas Channel are primarily due to changes in the relative proportion of the source waters; in contrast, local processes are likely more important in the three inlets. The larger range of salinity in Douglas Channel suggests that source waters experience less mixing by the time they reach the DC station compared with the stations in the southern fjords.

Further processes that require examination include the intensity and frequency of upwelling, and changes in deep water residence times and ventilation (e.g., Erlandson et al., 2006; Pawlowicz, 2017). Understanding these processes are important areas for future research.

5. Conclusions

An analysis of deep water from three British Columbia mainland fjords (Rivers, Knight and Bute Inlet) has found that from 1951 to 2020, temperature and salinity increased while oxygen decreased. In these three fjords, temperature warmed up to two times faster than the global average of waters at similar depths and these changes can be attributed to warming of offshore waters that are the source for fjord deep water via upwelling, and possibly continental warming that changed outflow winds. Decreased oxygen in offshore waters can also explain the lower oxygen in fjord deep water though it is likely that enhanced remineralization from warming further reduced oxygen in the fjords.

Douglas Channel was different. Although temperature warmed at the same rate as Rivers Inlet until at least 2016, oxygen did not decrease at a statistically significant rate. An analysis of AOU versus S suggests that deep waters in Douglas Channel are more readily exchanged with the outer coast than the three other fjords.

Data Availability Statement

All data used in this project are managed by CIOOS and can be found at https://catalogue.cioos.ca/en/harvest/cioos-pacific

Acknowledgments
Funding for this research was provided by the Tula Foundation (J. M. Jackson, and J. Barrette) and Fisheries and Oceans Canada (L. Bianucci and C. G. Hannah). We thank the scientists and crew from the University of British Columbia, Fisheries and Oceans Canada, and the Hakai Institute for collecting these data. Keith Holmes created Figure 1. We gratefully acknowledge that this work took place on the traditional territories of the Gitga'at, Wuikinuxv, Tlowitsis, Da'naxda'xw Awaetlala, and Homalco First Nations. This research is not associated with any known conflict of interest. We thank the editor and two reviewers for their constructive comments, which improved this manuscript.

References

Aksnes, D. L., Aure, J., Johansen, P.-O., Johnsen, G. H., & Gro Vea Salvanes, A. (2019). Multi-decadal warming of Atlantic water and associated decline of dissolved oxygen in a deep fjord. *Estuarine, Coastal and Shelf Science*, *228*, 106392. https://doi.org/10.1016/j.ecss.2019.106392

Baker, P., & Pond, S. (1995). The low-frequency residual circulation in Knight Inlet, British Columbia. *Journal of Physical Oceanography*,*25*, 747–763. https://doi.org/10.1175/1520-0485(1995)025<0747:TLFRCI>2.0CO;2

Bianchi, T. S., Arndt, S., Austin, W. E. N., Benn, D. I., Bertrand, S., Cui, X., et al. (2020). Fjords as Aquatic Critical Zones (ACZs). *Earth-Science Reviews*, *203*, 103145. https://doi.org/10/1026/j.earscirev.2020.103145

Boone, W., Rysgaard, S., Carlson, D. F., Meire, L., Kirillov, S., Mortensen, J., et al. (2018). Coastal freshening prevents fjord bottom water renewal in Northeast Greenland: A mooring study from 2003 to 2015. *Geophysical Research Letters*, *45*, 2726–2733. https://doi.org/10.1002/2017GL076591

Brewer, P. G., & Peltzer, E. T. (2017). Depth perception: The need to report ocean biogeochemical rates as functions of temperature, not depth. *Philosophical Transactions of the Royal Society A: Mathematical, Physical and Engineering Sciences*, *375*, 20160319. https://doi.org/10.1098/rsta.2016.0319

British Columbia. Ministry of Environment (2016). *Indicators of climate change for British Columbia, 2016 update*, Victoria, BC: eBook. https://www2.gov.bc.ca

Broecker, W. S., & Peng, T. H. (1982). *Tracers in the sea, Lamont-Doherty Earth Observatory*. NY, U.S.A: Palisades.

Chandler, P. C., Foreman, M. G. G., Ouellet, M., Mimeault, C., & Wade, J. (2017). Oceanographic and environmental conditions in the Discovery Islands, British Columbia. *DFO Canadian Science Advisory Secretariat Research Document*, *071*(XIII), 51. https://waves-vagues.dfo-mpo.gc.ca/Library/40653043.pdf

Crawford, W. R., & Peña, M. A. (2016). Decadal trends in oxygen concentration in subsurface waters of the Northeast Pacific Ocean. *Atmosphere-Ocean*, *54*(2), 171–192. https://doi.org/10.1080/07055900.2016.1158145

Cummins, P. F., & Ross, T. (2020). Secular trends in water properties at Station P in the northeast Pacific: An updated analysis. *Progress in Oceanography*, *186*, 102329. https://doi.org/10.1016/j.pocean.2020.102329

Diaz, R. J., & Rosenberg, R. (2008). Spreading dead zones and consequences for marine ecosystems. *Science*, *321*, 5891926–5891929. https://doi.org/10.1126/science.1156401

Erlandsson, C. P., Stigebrandt, A., & Arneborg, L. (2006). The sensitivity of minimum oxygen concentrations in a fjord to changes in biotic and abiotic external forcing. *Limnology and oceanography*, *51*(1, part 2), 631–638. https://doi.org/10.4319/lo.2006.51.1_part_2.0631

Farmer, D. M., & Freeland, H. J. (1983). The physical oceanography of fjords. *Progress in Oceanography*, *12*(2), 147–219. https://doi.org/10.1016/0079-6611(83)90004-6

Freeland, H. J. (2013). Evidence of change in the winter mixed layer in the Northeast Pacific Ocean: A problem revisited. *Atmosphere-Ocean*, *51*(1), 126–133. http://dx.doi.org/10.1080/07055900.2012.754330

Hare, A., Evans, W., Pocock, K., Weekes, C., & Giminez, I. (2020). Contrasting marine carbonate systems in two fjords in British Columbia, Canada: Seawater buffering capacity and the response to anthropogenic CO2 invasion. *PLoS One*, *15*(9), e0238432. https://doi.org/10.1371.journal.pone.0238432

Hodal, M. (2010). *Net physical transports, residence times, and new production for Rivers Inlet* (MSc thesis, p. 71). BC: University of British Columbia. https://doi.org/10.14288/1.0053224

Ito, T., Follows, M. J., & Boyle, E. A. (2004). Is AOU a good measure of respiration in the oceans? *Geophysical Research Letters*, *31*(17), L17305. https://doi.org/10.1029/2004GL020900

Jackson, J. M., Johnson, G. C., Dosser, H. V., & Ross, T. (2018). Warming from recent marine heatwave lingers in deep British Columbia fjord. *Geophysical Research Letters*, *45*, 9757–9764. https://doi.org/10.1029/2018GL078971

Johnson, G. C., Lyman, J. M., Boyer, T., Cheng, L., Domingues, C. M., Gilson, J., et al. (2020). Ocean heat content [in "State of the Climate in 2019"]. *Bulletin of the American Meteorological Society*, *101*(8), S140–S144. https://doi.org/10.1175/BAMS-D-20-0105.1

Koeve, W., & Kähler, P. (2016). Oxygen utilization rate (OUR) underestimates ocean respiration: A model study. *Global Biogeochemical Cycles*, *30*, 1166–1182. https://doi.org/10.1002/2015GB005354

Lafond, C. A., & Pickard, G. L. (1975). Deepwater exchanges in Bute Inlet, British Columbia. *Journal of the Fisheries Research Board of Canada*, *32*, 2075–2089. https://doi.org/10.1139/f75-246

Laufkötter, C., John, J. G., Stock, C. A., & Dunne, J. P. (2017). Temperature and oxygen dependence of the remineralization of organic matter. *Global Biogeochemical Cycles*, *31*(7), 1038–1050. https://doi.org/10.1002/2017GB005643

Lomas, M. W., Glibert, P. M., Shiah, F. K., & Smith, E. M. (2002). Microbial processes and temperature in Chesapeake Bay: Current relationships and potential impacts of regional warming. *Global Change Biology*, *8*, 51–70. https://doi.org/10,1046/j.1365-2486.2002.00454.x

López-Urrutia, Á., Martin, E. S., Harris, R. P., & Irigoien, X. (2006). Scaling the metabolic balance of the oceans. *Proceedings of the National Academy of Sciences of the United States of America*, *103*, 8739–8744. https://doi.org/10.1073/pnas.0601137103

McNeil, M. R. (1974). *The mid-depth temperature minimum in B.C. Inlets*, Vancouver, B.C.: University of British Columbia. Retrieved from https://ocean.library.ubc.ca/collections/ubctheses/831/items/1.0053207

Narvaez, D. A., Vargas, C. A., Cuevas, L. A., Garcia-Loyola, S. A., Segura, C., Tapia, F. J., & Broitman, B. R. (2019). Dominant scales of subtidal variability in coastal hydrography of the Northern Chilean Patagonia. *Journal of Marine Systems*, *193*, 59–73. https://doi.org/10.1016/j.marsys.2018.12.008

Oliver, A. A., Tank, S. E., Giesbrecht, I., Korver, M. C., Floyd, W. C., Sanborn, P., et al. (2017). A global hotspot for dissolved organic carbon in hypermaritime watersheds of coastal British Columbia. *Biogeosciences*, *14*, 3743–3762. https://doi.org/10.5194/bg-14-3743-2017

Pawlowicz, R. (2017). Seasonal cycles, hypoxia, and renewal in a coastal fjord (Barkley Sound, British Columbia). *Atmosphere-Ocean*, *55*(4–5), 264–283. https://doi.org/10.1080/07055900.2017.1374240

Peña, M. A., Masson, D., & Callendar, W. (2016). Annual plankton dynamics in a coupled physical–biological model of the Strait of Georgia, British Columbia. *Progress in Oceanography*, *146*, 58–74. https://doi.org/10.1016/j.pocean.2016.06.002

Pickard, G. L. (1961). Oceanographic features of inlets in the British Columbia mainland coast. *Journal of the Fisheries Research Board of Canada*, *18*(6), 908–999. https://doi.org/10.1139/f61-062

Pomeroy, L. R., & Wiebe, W. J. (2001). Temperature and substrates as interactive limiting factors for marine heterotrophic bacteria. *Aquatic Microbial Ecology*, *23*, 187–204. https://doi.org/10.3354/ame023187

Pytkowicz, R. M. (1971). On the apparent oxygen utilization and the preformed phosphate in the oceans. *Limnology and Oceanography*, *16*(1), 39–42. https://doi.org/10.4319/lo.1971.16.1.0039

Scannell, H. A., Johnson, G. C., Thompson, L., Lyman, J. M., & Riser, S. C. (2020). Subsurface evolution and persistence of marine heatwaves in the northeast Pacific. *Geophysical Research Letters*, *47*, e2020GL090548. https://doi.org/10.1029/2020GL090548

Segschneider, J., & Bendtsen, J. (2013). Temperature dependent remineralization in a warming ocean increases surface pCO2 through changes in marine ecosystem composition. *Global Biogeochemical Cycles*, *27*(4), 1214–1225. https://doi.org/10.1002/2013GB004684

Silva, N., & Vargas, C. A. (2014). Hypoxia in Chilean Patagonian Fjords. *Progress in Oceanography*, *129*, 62–74. https://dx.doi.org/10.1016/j.poceam/2014.05.016

St. Pierre, K. A., Oliver, A. A., Tank, S. E., Hunt, B. P. V., Giesbrecht, I., Kellogg, C. T. E., et al. (2020). Terrestrial exports of dissolved and particulate organic carbon affect nearshore ecosystems of the Pacific coastal temperature rainforest. *Limnology and Oceanography*, *65*, 2657–2675. https://doi.org/10.1002/lno.11538

Wan, D., Hannah, C. G., Foreman, M. G. G., & Dosso, S. (2017). Subtidal circulation in a deep-silled fjord: Douglas Channel, British Columbia. *Journal of Geophysical Research*, *122*, 4163–4182. https://doi.org/10.1002/2016JC012022